ISSN 0742-0463, Journal of Volcanology and Seismology, 2010, Vol. 4, No. 6, pp. 396–411. © Pleiades Publishing, Ltd., 2010.
Original Russian Text © Yu.F. Kopnichev, I.N. Sokolova, 2010, published in Vulkanologiya i Seismologiya, 2010, No. 6, pp. 34–51.

On the Correlation between Seismicity Characteristics and S-Wave Attenuation in the Ring Structures that Appear before Large Earthquakes

Yu. F. Kopnichev[a] **and I. N. Sokolova**[b]

[a] *Schmidt Institute of Physics of the Earth, Russian Academy of Sciences, Moscow, 123995 Russia*
e-mail:yufk@kndc.kz

[b] *Institute of Geophysical Research, Nuclear Science Center, Republic of Kazakhstan, Alma-Ata, 050020*
e-mail:sokolova@kndc.kz

Received July 4, 2008

Abstract—We discuss seismicity characteristics in the source zones of two great earthquakes: the December 26, 2004 Sumatra ($M_w = 9.0$) and the November 14, 2001 Kunlun ($M_w = 7.8$) events. Ring structures of low magnitude seismicity have been forming prior to these earthquakes for several decades. We studied the short period shear-wave attenuation field in the area of these ring structures. The method we used is based on the analysis of the rate of attenuation for the early Sn and Lg codas to detect attenuation inhomogeneities in the uppermost mantle. We show that the ring structures have comparatively high attenuation of shear waves compared with the crustal volumes inside the rings. The fact that there is no recent volcanism in the area of the seismicity rings shows that this effect is due to a high content of free fluids in the uppermost mantle. Proceeding by analogy with our results, we identified a zone in northern Tien Shan that is anomalous for these parameters; the zone may be related to the precursory process of a large earthquake. We discuss the geodynamic mechanisms that may be responsible for fluid concentration in the seismicity rings.

DOI: 10.1134/S0742046310060047

INTRODUCTION

It is known that many large earthquakes in various regions worldwide were preceded by ring structures of seismicity, which generally take several decades to form [Sobolev, 1993; Kopnichev and Mikhailova, 2000; Kopnichev et al., 2006; Jaume and Sykes, 1999]. Such structures mostly consist of earthquakes with energies a few orders below that of the main shocks [Sobolev, 1993; Kopnichev et al., 2006; Jaume and Sykes, 1999]. These facts are of importance for predicting the locations of future large earthquakes, but the origin of these ring structures remains poorly understood [Jaume and Sykes, 1999]. It is therefore of great interest to study the fine structure of the Earth's crust and uppermost mantle in the areas of such seismicity rings, primarily for the identification of fluid-rich zones, since recent studies have shown the very important part played by free lithospheric fluids in the precursory processes of large earthquakes [Kopnichev and Mikhailova, 2000; Kasahara et al., 2001; Yamasaki and Seno, 2003]. One of the most effective parameters that help to detect fluid-rich zones is the attenuation of short period shear waves, which are very sensitive to the presence of a liquid phase [Kopnichev and Mikhailova, 2000; Kopnichev and Sokolova, 2000, 2003, 2007; Kopnichev et al., 2004, 2006, 2009]. The present study compares seismicity characteristics and shear wave attenuation in the source zones of two great earthquakes, the December 26, 2004 Sumatra, $M_w = 9.0$ and the November 14, 2001 Kunlun, $M_w = 7.8$ events. Proceeding by analogy with the data we obtained, we identified a zone that is anomalous by these parameters in northern Tien Shan where no $M > 6.5$ earthquakes have occurred during the last several centuries.

METHOD OF STUDY

Identification of ring structures of seismicity. The first stage of this work involved examination of seismicity in the area of study, which includes the source zone of a large earthquake. We made maps of the epicenters of earthquakes with magnitudes equal to or greater than a threshold value (Mthre) where Mthre was usually 2–3 magnitude units below the mainshock magnitude. The seismicity rings were constructed so as to have approximately equal numbers of comparatively smaller events on both sides of the ring outline. In nearly all cases that were considered in previous studies, the rings had shapes close to an ellipse [Sobolev, 1993; Kopnichev and Mikhailova, 2000; Kopnichev et al., 2006; Jaume and Sykes, 1999]. It should be noted that the ring structures become "hazy," when the values of Mthre are too low [Jaume and Sykes, 1999]. We used post-1964 earthquakes, because earthquake location accuracy was enhanced thanks to the appearance of the worldwide standardized seismographic network, WWSSN [Butler et al., 2004]. For Sumatra and Tibet we analyzed data from the NEIC since 1973 (www.earthquake.usgs.gov) and from the ISC for 1964–1972 (www.isc.ac.uk); for central Tien Shan the catalog was SOME MON RK (www.kndc.kz).

Mapping the attenuation field. This was done using a method based on the analysis of the rate of decay for the early Sn and Lg coda amplitudes; the method estimates the overall attenuation in the uppermost mantle around the epicenter from the data of a single station [Kopnichev et al., 2009].

We considered the envelopes of Lg and Sn codas due to comparatively small earthquakes (usually with $M < 5.5$). The crustal Lg phase is a combination of overcritical shear-wave reflections at the crustal bottom; its average velocity is very stable in different areas and is close to 3.5 km/s [Kopnichev, 1985; Kaazik et al., 1990]. The Lg group disappears when the path traverses oceanic crust, as well as when the attenuation in continental crust is sufficiently high. In such cases the records only show the Sn group with its coda, which penetrates the upper mantle (Fig. 1) [Kopnichev, 1985; Kopnichev and Arakelyan, 1988].

Several works [Kopnichev, 1985; Kopnichev and Arakelyan, 1988; Kaazik et al., 1990] have thoroughly studied coda characteristics at frequencies around 1 Hz (including the analysis of arrival direction and apparent velocities, polarization, space–time variations, etc.). The analysis suggests that the Sn and Lg codas have a similar origin; they are mostly composed of shear reflections from numerous subhorizontal interfaces in the upper mantle.

As lapse time *t* since the radiation began increasesing, the coda receives waves that were incident at the crustal bottom at progressively higher angles and penetrate to greater depths in the upper mantle. Figure 1 shows a schematic diagram of the rays that make up the Sn and Lg codas. Ray I is a head wave that propagates along the Moho. The later arrivals are shear waves that are reflected at various interfaces in the upper mantle. If the source zone in the uppermost mantle involves a zone of relatively lower (higher) attenuation, this will lead to a comparatively slower (faster) decay of amplitudes in the initial part of the coda (rays II and III). After ray III come shear waves, which penetrate into the volume of "normal" (for the depth range involved) attenuation. This gives a rapid increase or decrease, respectively, in the rate of decay of coda amplitudes. The resolution of this method is a few tens of kilometers [Kopnichev et al., 2009].

Since attenuation significantly depends on frequency [Kopnichev, 1985], we began by performing narrowband filtering of the vertical components. We used a filter centered at 1.25 Hz; it was 2/3 octaves wide. The formula $Ac(t) \sim \exp(-\pi t/QsT)/t$ (Ac is coda amplitude, T the period [Kopnichev, 1985; Kopnichev et al., 2009]) was used to determine effective Q in the time interval 70 s following Lg (between t = 100–170 s at epicentral distance $\Delta \sim 250$ km and t = 330–400 s at $\Delta \sim 1100$ km). Estimates show that the ray offsets at depths down to 100 km is several tens of kilometers for waves that correspond to the end-points of these intervals (the depth of focus was assumed to be zero) [Kopnichev et al., 2009]. When there was no 1-Hz Lg group on the records, measurements were made after the time of its theoretical arrival as given by the time–distance curve. We wish to note that effective Qs

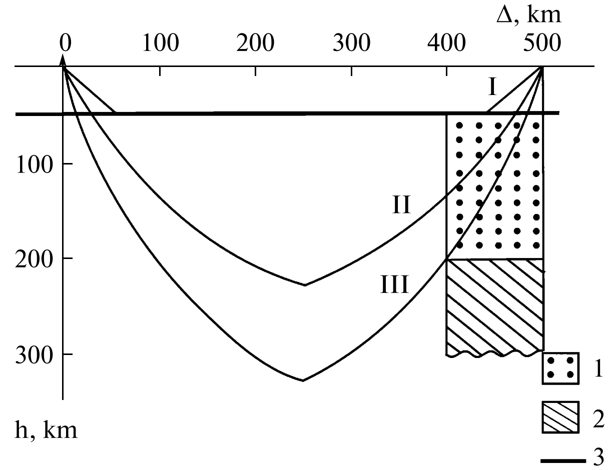

Fig. 1. Diagram of rays that form the Lg and Sn codas: (1) volume of anomalous attenuation in the upper mantle, (2) volume of "normal" attenuation, (3) Moho interface.

incorporates the overall effect of attenuation proper (absorption) and scattering [Kopnichev, 1985]. However, as has been shown previously, the relation $\alpha a/\alpha s \gg 1$ holds for frequencies of ~1 Hz, even in areas of comparatively low seismic attenuation in the upper mantle, where αa and αs are the attenuation and scattering coefficients, respectively [Kopnichev, 1985]. Numerical simulation corroborates this observation [Kaazik and Kopnichev, 1990]. With this result in mind, we can assume that Qs is mostly due to shear wave attenuation in all cases considered. Unlike [Kopnichev et al., 2009], we did not determine the Q in the distant code, which was used for normalization when comparing data acquired in very different areas. This allowed us to use records of comparatively small events for our analysis.

DATA ANALYSIS

The zone of the December 26, 2004 Sumatra earthquake. This event, the greatest in the world since 1964, caused a giant tsunami in the Indian Ocean. The aftershock area was about 1400 km long. It was a thrust earthquake, a mechanism typical of great earthquakes at subduction zones [Rhie et al., 2007].

Figure 2 shows the epicenters of all shallow ($h \leq 33$ km) moderate-sized ($M \geq 5.5$) earthquakes that occurred in the southern part of the source zone and its environs during the period from January 1, 1969 to December 25, 2004. One can see that a ring structure is formed in the area between 1° and 7°N by the epicenters; the greater axis of the structure is about 700 km and strikes northwest. The Sumatra earthquake epicenter is near the eastern edge of the ring. It should be noted that the overwhelming part of the larger aftershocks of this event at depths of 34–60 km, which were recorded prior to March 28, 2005, when another great earthquake ($M_w = 8.6$) occurred in the Sumatra region, were confined to the boundary of the structure (see Fig. 2).

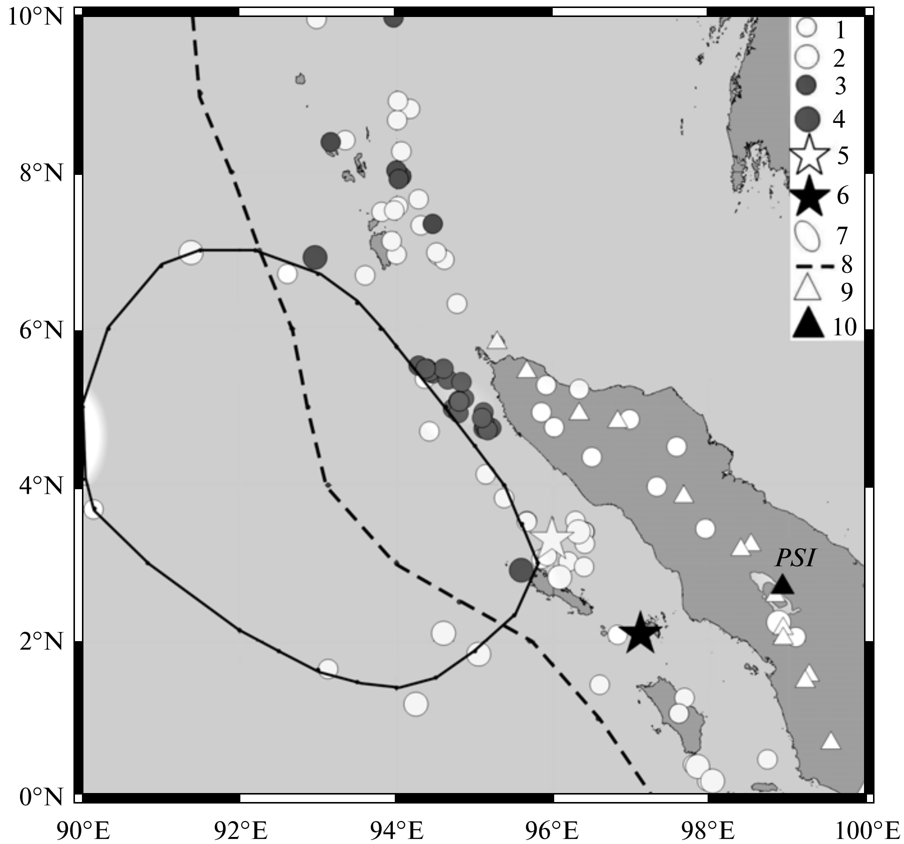

Fig. 2. Seismicity characteristics in the source zone of the Sumatra earthquake. The period January 1, 1964 to December 25, 2004: (1, 2) depths of 0–33 km and the period December 26, 2004 to March 27, 2005: (3, 4) depths of 34–60 km. (1, 3) $5.5 \le M < 6.5$, (2, 4) $M \ge 6.5$, (5, 6) the epicenters of the December 26, 2004 and March 28, 2005 earthquakes ($M_w = 8.6$), respectively, (7) seismicity ring before the December 26, 2004 Sumatra earthquake, (8) trench axis, (9) volcanoes, (10) seismic station.

Figure 3 shows the values of M versus time for the earthquakes in the ring area for the period between 1964 and 2004. From this figure it follows that the rate of $M \ge 5.5$ events began increasing rapidly from 1994. Two rather large events occurred during the last decade prior to the 2004 Sumatra earthquake (November 8, 1995 with M = 7.1 and November 2, 2002 with M = 7.6). From this it follows that the mean rate of seismotectonic strain in the ring structure area reached its maximum approximately 2 years before the main shock.

Our study of inhomogeneities in the attenuation field was based on records of shallow earthquakes ($h \le 30$ km) made at the PSI station (mostly in 2004–2006) at epicentral distances of ~250–700 km. (We note that the thickness of continental crust in the Sumatra I. area is about 30 km [Simoes et al., 2004].) More than 200 records of $M \le 5.5$ events were used.

Figure 4 shows sample records of two crustal earthquakes made at the *PSI* station. The earthquake epicenters are inside the seismicity ring and at its boundary. From this figure it follows that the earlier Sn coda for the first event (in a time interval of ~70–80 s duration) decayed much more slowly than that for the second.

Figure 5 shows examples of the general coda envelope for different parts of the source zone and its environs. It can be seen that the rate of decay for the amplitudes in the earlier coda is subject to considerable variation. In the case under consideration, the gentle slope in the initial part of the coda corresponds to the area of the deep-sea trench and to that east of the volcanic front. A much steeper slope is observed for the volcanic area. It should be noted that the highest attenuation of coda amplitudes for this line corresponds to the area west of Sumatra I. at distances of about 180 km from the trench.

Figure 6 shows the attenuation field in the area of study. The entire range of Qs is divided into three levels corresponding to high (Qs = 150–220), intermediate (230–330), and low (370–1000) attenuation. Each symbol is referred to the center of a small zone (generally a few tens of kilometers in diameter) for which we constructed the overall coda envelopes, and, thus, averaged the data. One can see two linear bands of high attenuation trending northwest and north–northeast between the trench and Sumatra I. The epicenter of the Sumatra earthquake is in the area where the two bands intersect. It is important to note that the eastern part of the shallow seismicity ring is

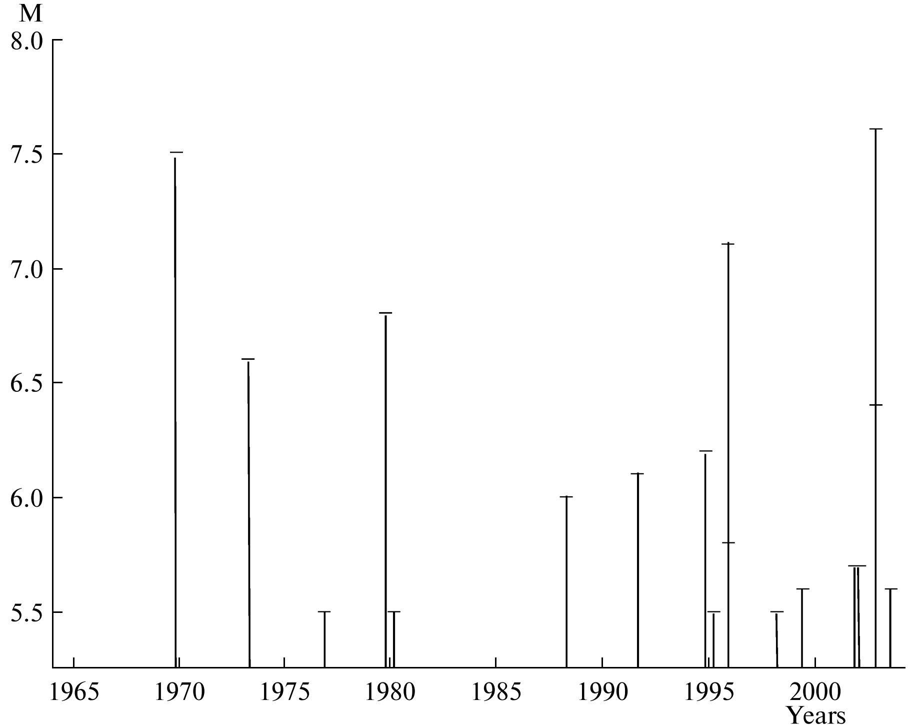

Fig. 3. Distribution of earthquake magnitudes over time in the area of a ring structure.

confined to the northwestern and southwestern parts of the bands. It is of interest that the southwestern edge of the southern band of high attenuation intersects the trench. The attenuation shows a dramatic drop northwest of it. One mostly has low and intermediate attenuation inside the seismicity ring. A narrow zone of intermediate Qs is on the west boundary of Sumatra I. The attenuation field is very heterogeneous east of that zone, in the volcanic area. We note that the attenuation is low in the area of the northernmost Pleistocene volcano Poulau Weh, while the southern younger volcanoes (Seulawah Agam, Geureudong, and Peuet Sague) which erupted in the 19th–20th centuries, show high and partly intermediate attenuation. East of the volcanic front (between 97° and 98°N) the values of Qs rapidly increase.

Figure 7 shows the effective Q as a function of the distance for a line normal to the trench (see Fig. 6). The overall trend is for Qs to decrease from the trench toward the volcanic front. Upon this background we see a prominent anomaly in Qs where the high attenuation band is traversed (at distances of ~130–200 km from the trench). Overall, the values of Qs are even lower there than in the volcanic area.

The above data demonstrate a high shear wave attenuation in the uppermost mantle confined to the eastern and southeastern boundaries of the seismicity ring preceding the Sumatra earthquake.

The zone of the November 14, 2001 Kunlun earthquake. This earthquake occurred in northern Tibet and was the greatest in Central and South Asia, second only to the 1950 Assam earthquake. The faulting was right lateral strike–slip; the surface breakage extended for about 400 km [Bufe, 2004] (Fig. 8). The rupture propagated from west to east [Bufe, 2004].

Figure 8 also shows the seismicity of the area within the coordinates 31–40°N and 85–95°E in Central Asia. We selected all $M \geq 5.5$ earthquakes for the period from January 1, 1964 to November 13, 2001. It follows from this figure that the overwhelming part of all events forms a ring whose greater axis extends north–northeast for about 700 km. The Kunlun earthquake epicenter is inside the ring at a distance of ~150 km from its eastern boundary.

Figure 9 illustrates the distribution of earthquakes in the area of this ring structure during the time period 1964–2001. In the case under consideration we see that 5 of the 19 $M \geq 5.5$ earthquakes, including the great ($M = 7.5$) earthquake of November 8, 1997, occurred between 1994 and 1997. It can thus be said that the seismicity ring mostly formed about 4 years prior to the main event.

Records from the *LSA* and *WMQ* stations were used to investigate inhomogeneities in the attenuation field in the area of study; a total of about 170 records of crustal earthquakes in the ranges of epicentral distance 330–730 and 550–1100 km, respectively, were used for *LSA* and *WMQ*. Figure 10 shows examples of *WMQ* records. It follows from this figure that the early Lg coda for the epicenter at the boundary of the ring structure in the time interval ~60–70 s decays much faster than outside the structure. Figure 11 shows Sn coda envelopes for the southern part of the study area based on *LSA* records. It can be seen that

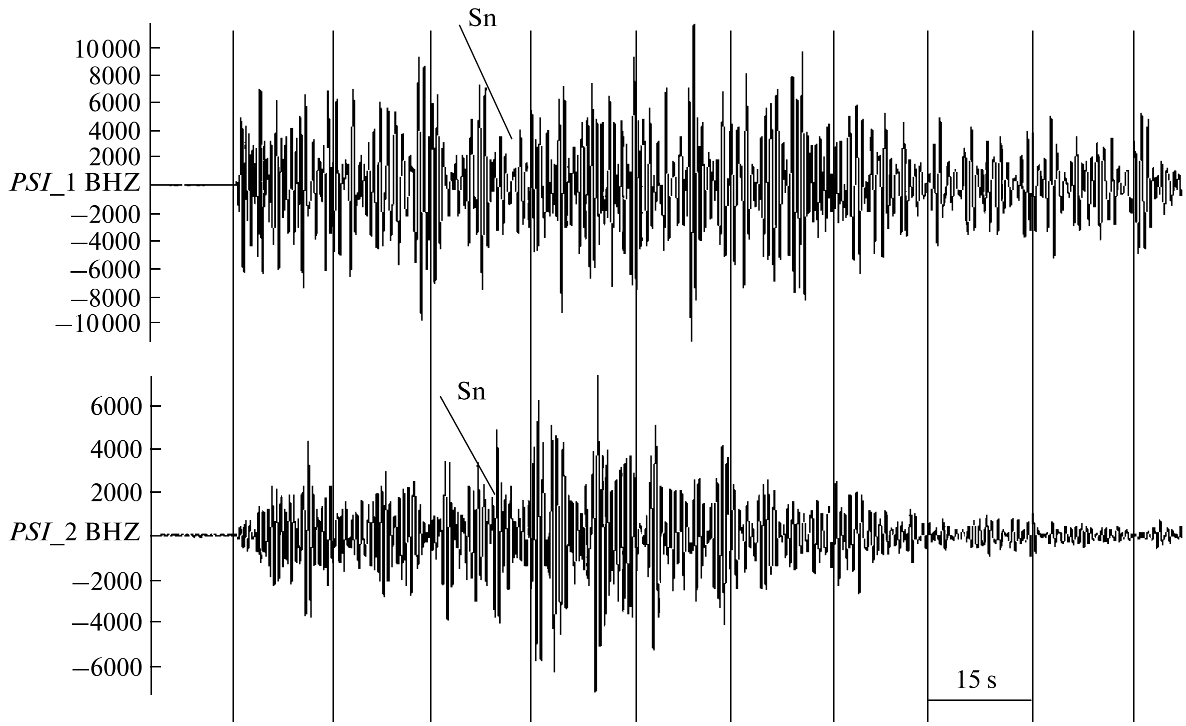

Fig. 4. Sample seismograms of earthquakes recorded at the *PSI* station. Here and below: a 1.25 Hz filter. The top trace is for an earthquake inside the seismicity ring (2.88°N and 95.46°E, h = 25 km, Δ = 385 km). The bottom trace is for an earthquake in the ring area (3.79°N and 95.80°E, h = 30 km, Δ = 367 km). Here and in Figs. 10 and 15 we indicate the arrivals of Sn and Lg and the time scale.

the envelopes have a much steeper slope in the initial part for epicenters at the ring boundary compared with zones inside and outside the ring.

Figure 12 shows a map of the attenuation field for the area of study. The data for each station were again divided into three grades corresponding to high (Qs = 120–150 and 190–260), intermediate (160–200 and 270–310), and low (210–300 and 340–420) attenuation for *LSA* and *WMQ*, respectively. We note that this large difference in Qs for the two stations is due to some features in the structure of the lithosphere and asthenosphere where the stations are installed, viz., in East Tien Shan (*WMQ*) the shear wave attenuation in the crust and upper mantle is much lower than in Tibet (*LSA*).

It follows from Fig. 12 that the symbols that denote high attenuation are concentrated at the boundary of the ring structure based on the *LSA* data. At the same time we see intermediate and low attenuation inside and outside the ring. The *WMQ* data show considerable variations in the attenuation field at the north boundary of the ring, zones of low, intermediate, and even high attenuation zones are identified. Nevertheless, the areas inside and outside of the ring (except for the 2001 rupture zone) mostly show intermediate and partly low attenuation.

The records of these stations were also used to map the source zone of the Kunlun earthquake. It appears from Fig. 12 that a prominent anomaly of high attenuation occurs in most of the source zone, both inside and outside of the ring, as inferred from the 1990–2004 *WMQ* data. At the same time, the source zone itself shows intermediate attenuation based on the *LSA* data.

It should be noted that nearly all major fault zones in Tibet trend roughly east–west, in a similar manner to the 2001 Kunlun rupture zone [Tapponnier and Molnar, 1977]. From this it follows that in the case under consideration, the characteristics of the attenuation field in the area of the seismicity ring are not related in an unambiguous manner to the positions of the major crustal faults.

To sum up, the characteristics of the lithosphere in the areas of the ring structures that formed before great earthquakes in a subduction zone (Sumatra I.) and in an intracontinental area proved to be similar; in both of these cases, comparatively high shear wave attenuation in the uppermost mantle was confined to the seismicity rings.

Below we describe results from a comparison of seismicity characteristics and attenuation in an anomalous zone of Central Tien Shan that was identified previously [Kopnichev et al., 2004, 2006] where no large earthquakes have been recorded during the past several hundred years.

<u>Central Tien Shan.</u> Our analysis of seismicity is based on the time interval 1993–2007 in order to exclude the effects due to the August 19, 1992 Susamyr earthquake (M = 7.3), the greatest event in Central Tien Shan after the 1946 Chatkal earthquake (M = 7.5). We note that the overall level of seismicity experienced a dramatic drop

since 1993 in all of Tien Shan [Kondorskaya and Shebalin, 1977; Kopnichev et al., 2004]. While the rate of seismicity during the period from 1887 to 1992 was one M ≥ 7.0 earthquake every 7–8 years, there has been no such event during the last 18 years. In addition, there was also an obvious deficit in the rate of M ≥ 6.0 earthquakes compared with the average seismicity. All of this evidence points to the idea that a possible large earthquake (M ≥ 6.5) is likely to occur in Tien Shan in the near future [Kopnichev et al., 2004, 2006; Kopnichev and Sokolova, 2007].

Figure 13 shows the epicenters of all K ≥ 11.0 earthquakes in Central Tien Shan (40–44°N, 73–80°E) during the period from January 1, 1993 to July 1, 2007. The highest level of activity was exhibited during this time interval by the Kokshaal Range at the boundary with Tarim, where several M ≥ 6.0 events have occurred. West of Lake Issyk Kul we identified a ring structure between 75° and 76°E whose greater axis (~150 km) trends nearly east–west. The structure extends from the eastern boundary of the Kirgiz range to the eastern part of the Naryn Basin. We note that this high density of epicenters of comparatively large events at the southern boundary of the ring is unusual, since it occurs in the Naryn Basin, whose seismicity rate is comparatively low [Kondorskaya and Shebalin, 1977]. At the eastern boundary of the ring structure we have the December 25, 2006 Kochkor earthquake (M = 5.8), which was the greatest earthquake in Tien Shan in 2006.

It should be noted that the structure we described is not the only one in Central Tien Shan. For example, a seismicity ring with similar dimensions and shape can be identified southeast of Lake Issyk Kul between 77° and 79°E (see Fig. 13). We pay so much attention to the ring structure west of the lake because it was the most prominent in the area of study (see below).

Figure 14 shows the distribution of earthquakes with different energy classes over time in the area of the structure under study. One can see that the rate of events became much higher in 2004–2007. It may be supposed that most of this ring structure had formed before 2008.

The records of the *KKAR* station were used to investigate the shear wave attenuation field in the area of study. We used more than 130 records of crustal earthquakes in the range of epicentral distance 320–700 km.

Figure 15 shows several records of earthquakes whose epicenters were inside and at the boundary of the seismicity ring. It can be seen that the amplitudes in the initial

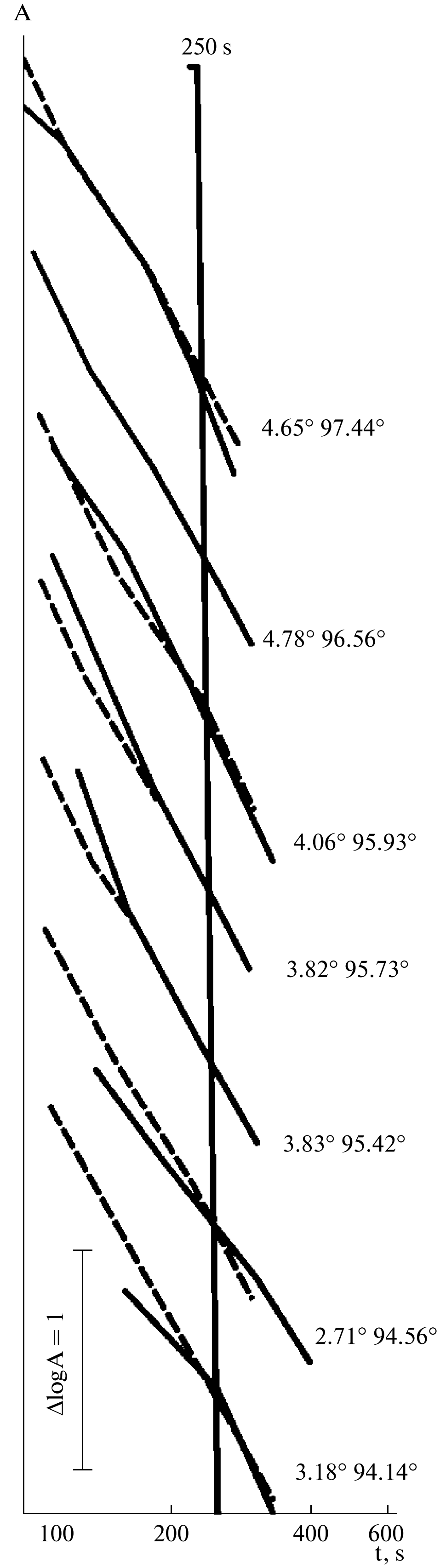

Fig. 5. Coda envelopes for different areas in the source zone and its immediate environs. The coordinates of the centers of the areas for which the overall envelopes were constructed are shown. From top to bottom: (1) beyond the volcanic front, (2 and the dashed line) the volcanic front, (3) between the volcanic front and the ring, (4, 5) the ring, (6, 7) inside the ring. The vertical line (here and in Figs. 11 and 16) corresponds to the time at which the envelopes were made to coincide.

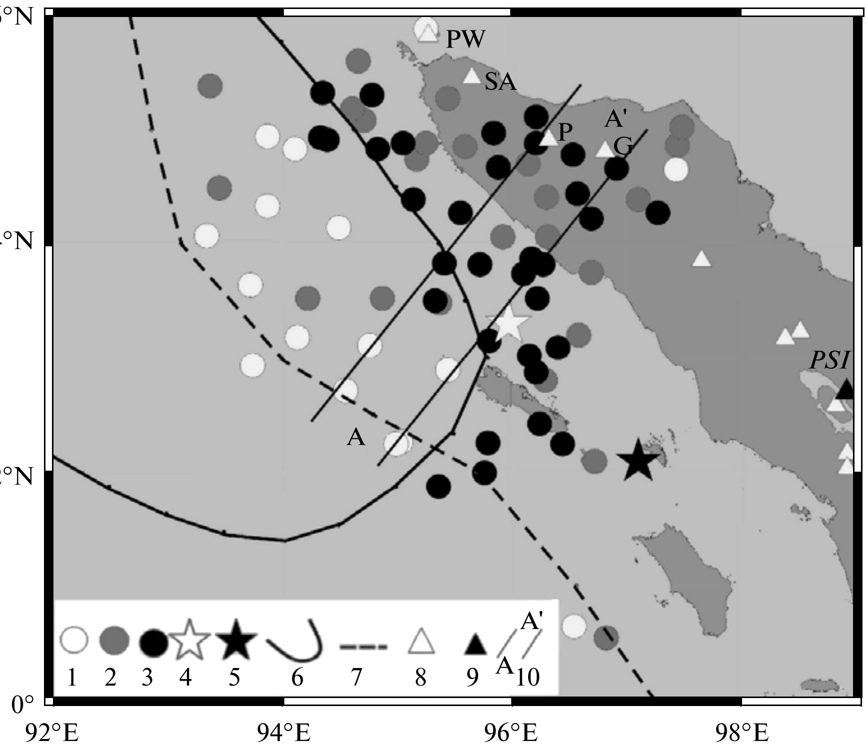

Fig. 6. Inhomogeneities in the shear wave attenuation field in the source zone of the Sumatra earthquake. Attenuation: (1) low, (2) intermediate, (3) high; (4, 5) the epicenters of the December 26, 2004 and March 28, 2005 earthquakes, respectively, (6) the seismicity ring before the December 26, 2004 earthquake, (7) trench axis, (8) volcanoes (we mark the ones that were mentioned in the main text): Poulau Weh (PW), Seulawah Agam (SA), Geureudong (G), and Peuet Sague (P), (9) seismic station, (10) line for which we consider effective Qs as a function of distance to trench.

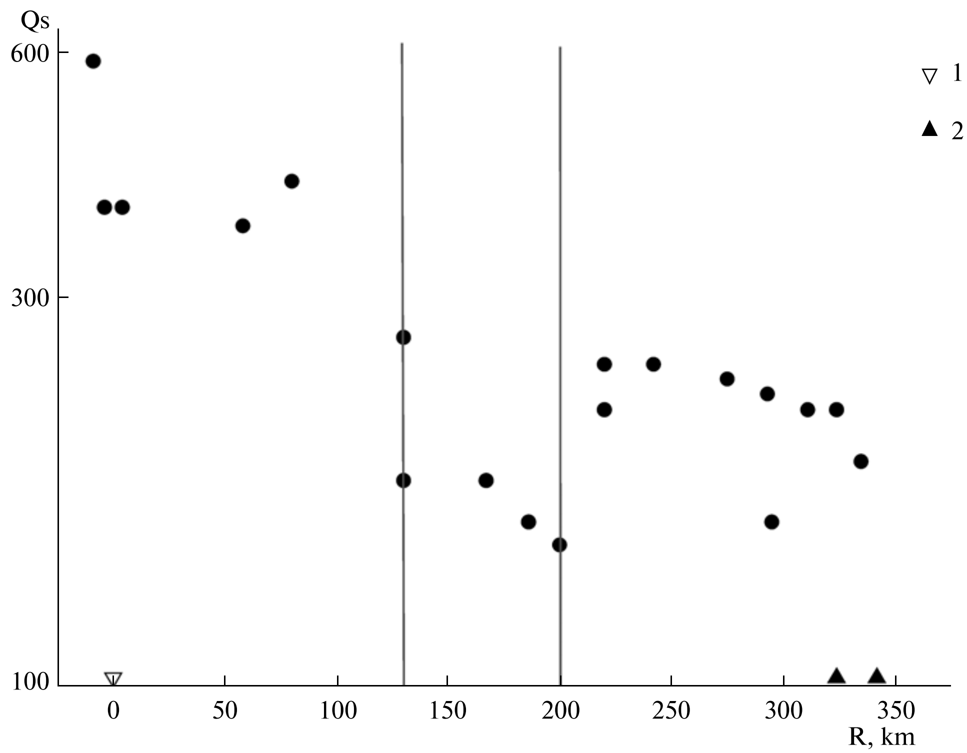

Fig. 7. The values of Qs in relation to the distance to trench for line A–A' (see Fig. 6): (1) trench axis, (2) volcanoes. Vertical lines mark the boundaries of the high attenuation band.

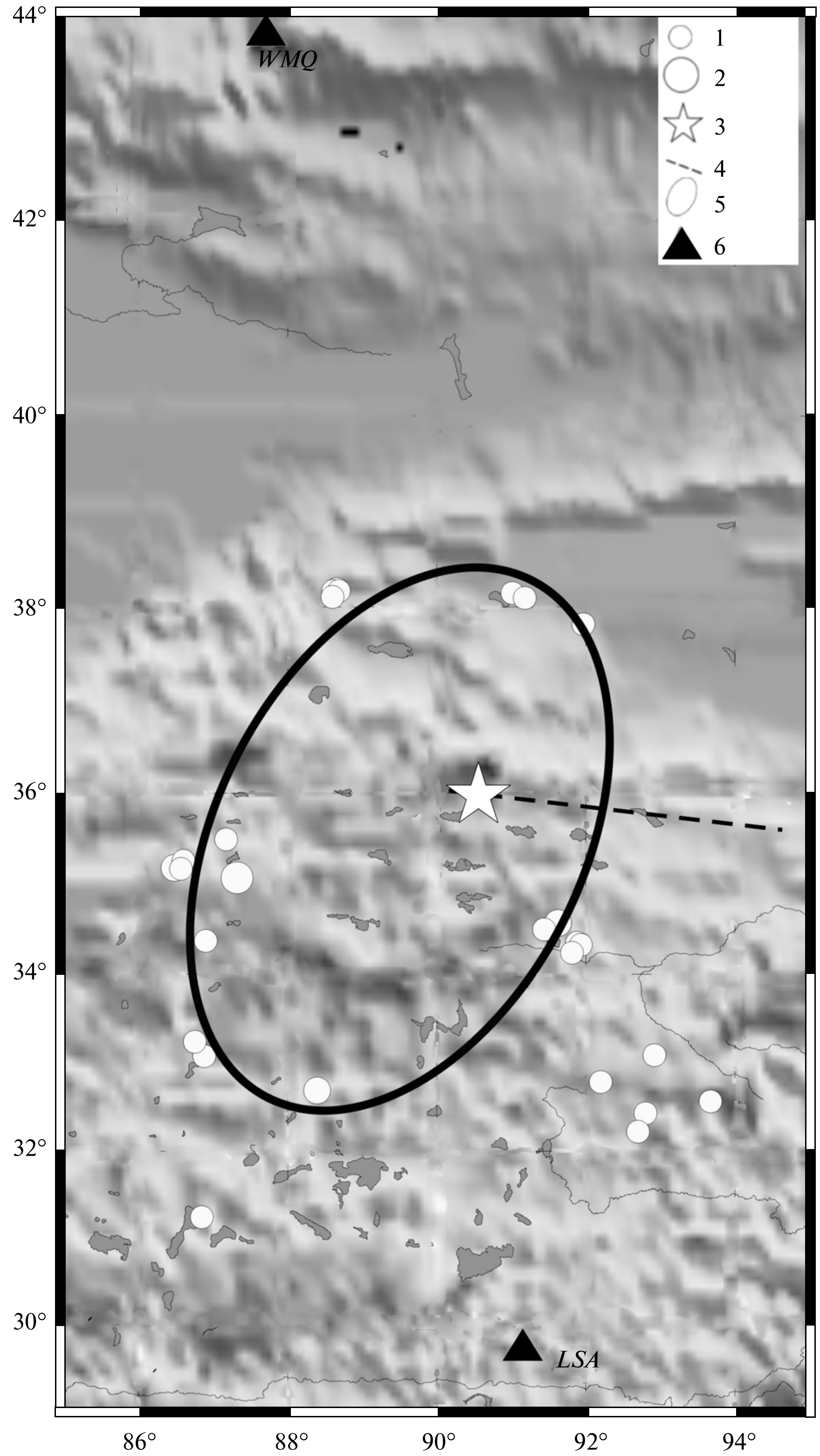

Fig. 8. Map of the area of study. Epicenters of large earthquakes: (1) $5.5 \leq M < 6.5$, (2) $M \geq 6.5$, (3) epicenter of the Kunlun earthquake, (4) positions of surface breakage due to the Kunlun earthquake, (5) seismicity ring, (6) seismic stations.

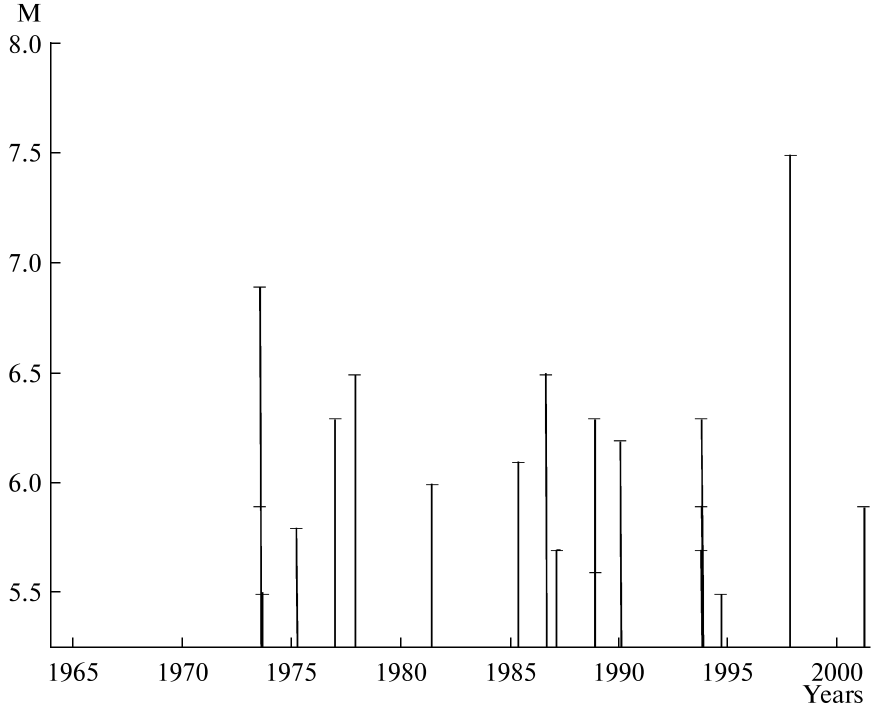

Fig. 9. Distribution of earthquake magnitudes over time in the ring structure area.

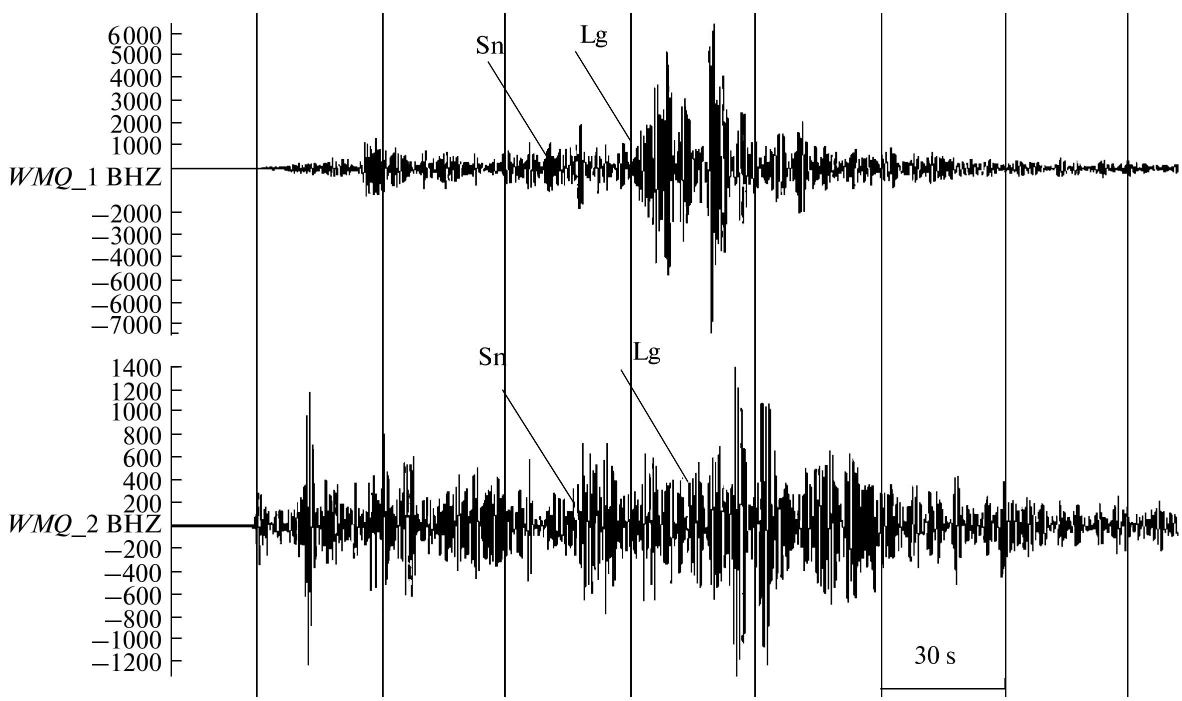

Fig. 10. Sample seismograms recorded at the *WMQ* station. The top trace is for an earthquake in the seismicity ring area (38.17°N, 88.69° E, h = 14 km, Δ = 632 km). The bottom trace is for an earthquake outside the ring (37.36°N, 86.76°E, h = 33 km, Δ = 722 km).

part of the Lg coda show a much faster falloff for the epicenter at the ring boundary.

Figure 16 illustrates the overall Lg coda envelopes constructed for a line that intersects the ring in the north–south direction. It follows from this figure that the slope of the early coda envelopes is much steeper for the zones at the ring boundary compared with the inside area and around the ring.

All values of effective Qs are divided into three levels corresponding to high (Qs = 220–290), intermediate (300–370), and low (390–1000 or greater) attenuation.

From the map in Fig. 17 it follows that most of the area shows intermediate and high values of Qs. Upon this background one can see a prominent anomaly of low Q confined to the ring structure. The centers of high attenuation zones are 0 to ~30 km distant from the ring boundary. The attenuation field is inhomogeneous in the ring area, as it is in Tibet, there being zones of intermediate Qs as well. Inside the ring we mostly have low and partly intermediate attenuation.

We note that all larger faults in the area of study trend east–west (the dominant Tien Shan direction), similarly to Tibet [Krestnikov et al., 1979]. It can thus be supposed that the characteristics of the attenuation field are not controlled by crustal faults in Central Tien Shan as well.

Figure 17 also shows the epicenters of the large ($M \geq 6.0$) earthquakes that have occurred in Western and Central Tien Shan between 1885 and 2007. It appears from this map that an east–west trending band of epicenters passes along the northern boundary of Central Tien Shan with two $M \geq 8.0$ events (the 1889 Chilik and the 1911 Kemin earthquakes). There is a gap in the western part of the band between the epicenters of the 1885 magnitude 6.9 Belovodskoe and the 1938 magnitude 6.9 Kemin earthquakes. It is important to note that this gap contains the northern boundaries of the seismicity ring and of the high attenuation zone. This area has not generated $M > 6.5$ earthquakes for about 500 years [Kondorskaya and Shebalin, 1977; Krestnikov et al., 1979]. Nevertheless, one can identify a zone of high density of paleoseismic ruptures capable of producing an earthquake of this size, which probably occurred in the 15th century [Kondorskaya and Shebalin, 1977; Krestnikov et al., 1979]. On the other hand, no $M > 6.5$ earthquakes are known to have occurred in the southern part of the ring structure (in the Naryn Basin) as can be concluded from instrumental, historical, and paleoseismic data [Kondorskaya and Shebalin, 1977; Krestnikov et al., 1979].

DISCUSSION

Large ring structures of seismicity that took several decades to form have been identified in the Sumatra area

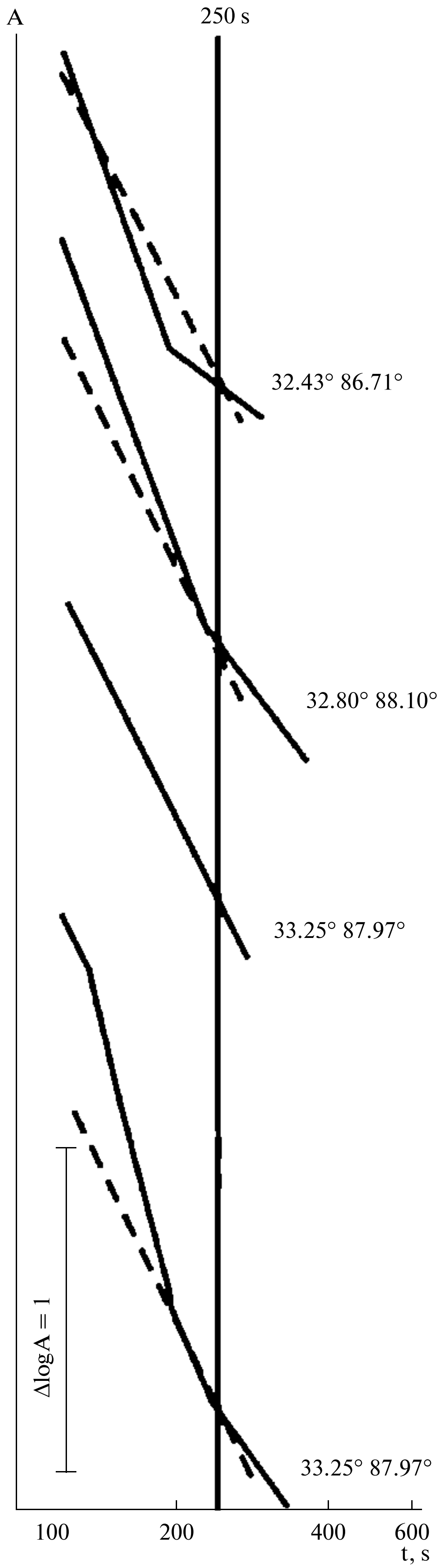

Fig. 11. Sample coda envelopes in the seismicity ring area. From top to bottom: (1) southwest of the ring, (2, 4) the ring, (3 and dashed line) inside the ring. The *LSA* station.

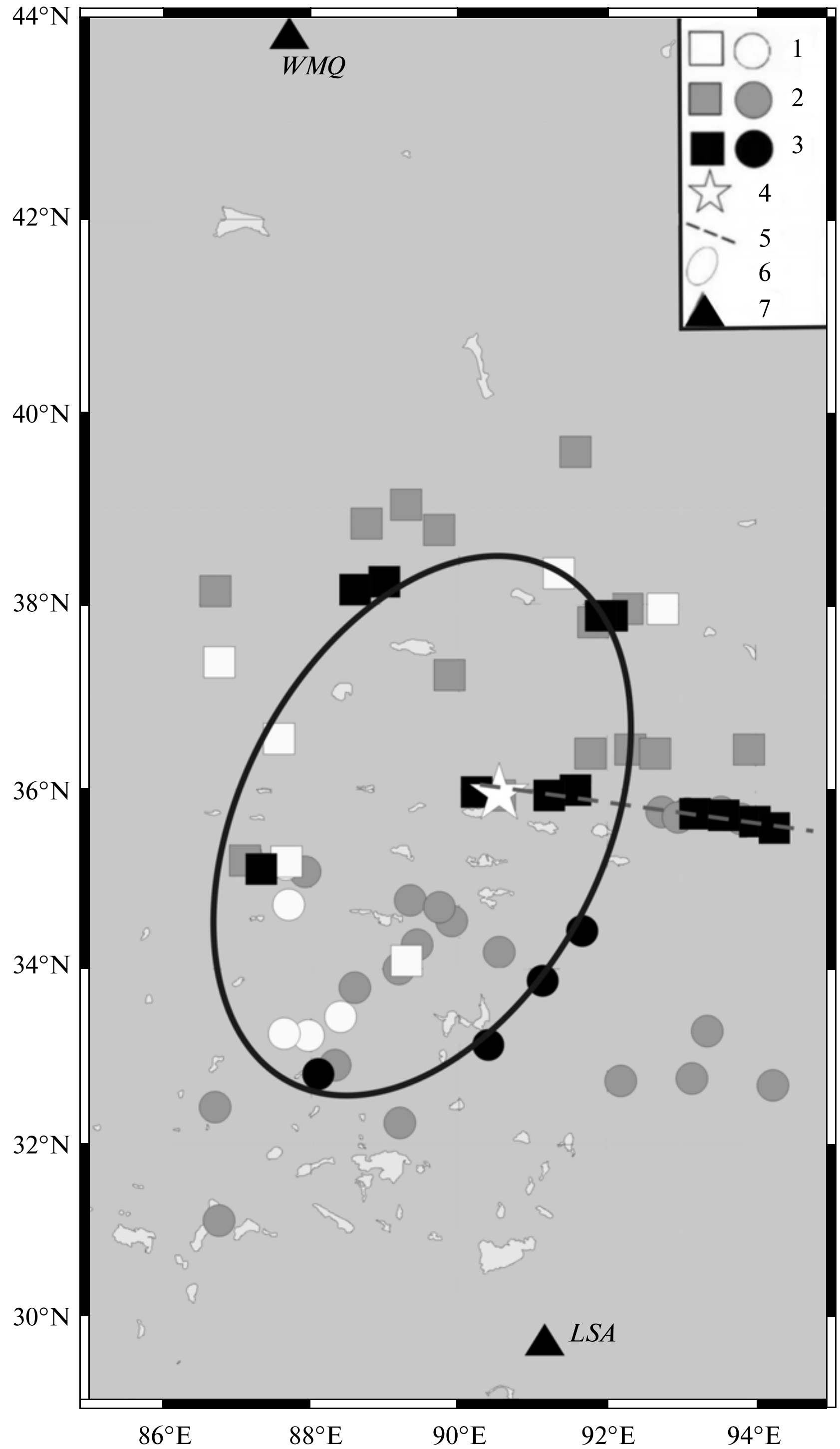

Fig. 12. Map of the attenuation field for Tibet. Attenuation: (1) low, (2) intermediate, (3) high (squares denote *WMQ* data, circles the *LSA* station), (4) epicenter of the Kunlun earthquake, (5) surface breakage due to the Kunlun earthquake, (6) seismicity ring, (7) seismic stations.

and in Tibet. The formation of these structures, which accelerated during the 7–10 years prior to great earthquakes, largely terminated a few years before these events. A similar, but much smaller seismicity structure was identified in Central Tien Shan where no M > 6.5 earthquakes have been recorded during the last several hundred years.

This study is the first to demonstrate that ring structures of seismicity have a corresponding high shear wave attenuation in the uppermost mantle. We note that high attenuation of short-period shear waves can occur when an appreciable percentage of partially molten material or fluids is present. However, there is no recent volcanism in

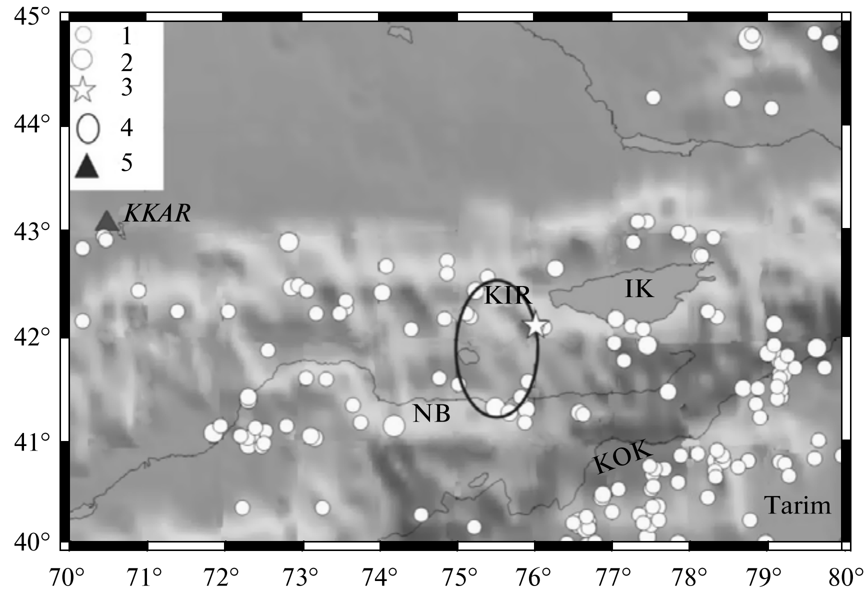

Fig. 13. A map of the study area. The epicenters of large earthquakes since 1993: (1) $11.0 \leq K < 12.0$, (2) $K \geq 12.0$; (3) epicenter of the December 25, 2006 Kochkor earthquake, (4) seismicity ring, (5) seismic station. The tectonic features occurring in the text: Kirgiz and Kokshaal ranges (KIR and KOK, respectively), Naryn Basin (NB), and Lake Issyk Kul (IK).

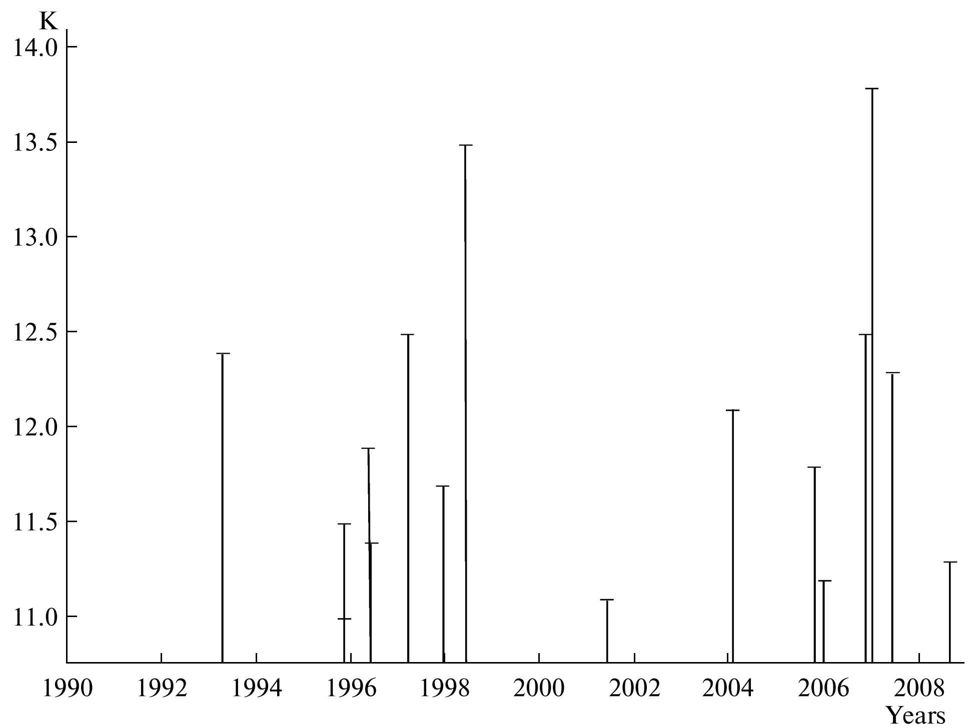

Fig. 14. Distribution of earthquake energy classes over time in the area of the ring structure.

all areas where we identified seismicity rings, which testifies to considerable presence of fluids.

The attenuation in a seismicity ring in a subduction zone (Sumatra I.) proved to be even higher than in a volcanic area. This testifies to considerable content of free fluids in the mantle wedge and in the plunging oceanic plate. This inference is also corroborated by the fact that most of the larger, relatively deep aftershocks are confined to the seismicity ring that formed prior to the Sumatra earthquake. (The aftershocks may have been due to embrittlement of upper mantle material due to dehydration [Nakajima and Hasegawa, 2006; Yamasaki and Seno, 2003].)

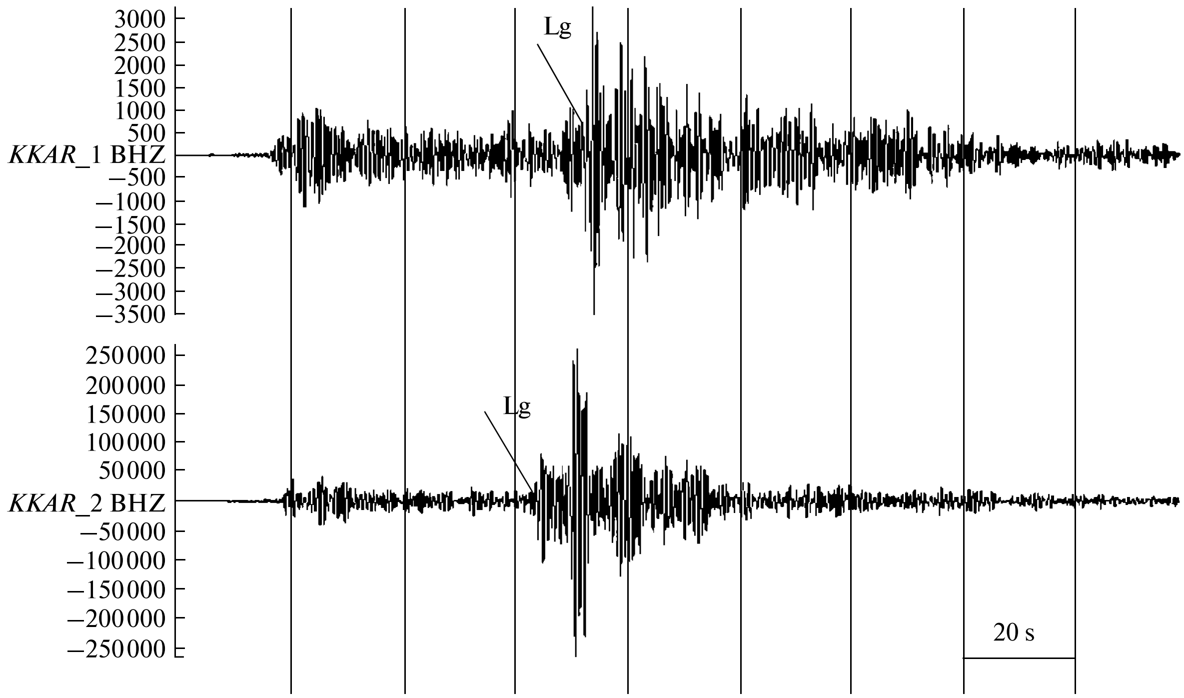

Fig. 15. Sample seismograms of earthquakes recorded by *KKAR*. Top trace is for an epicenter inside the ring (41.67°N, 75.35°E, h = 10 km, Δ = 444 km). Bottom trace is for an epicenter in the ring area (42.56°N, 75.28°E, h = 5 km, Δ = 380 km).

We also note that the high attenuation band that extends northwest corresponds to the position of the zone that shows the greatest rate of crustal uplift between the trench and the volcanic front that was observed before the 2004 earthquake [Simoes et al., 2004].

Judging from the available data, the zone of high attenuation in the southeastern part of the seismicity ring in the Sumatra area is nearly continuous in a band ~500 km long and ~70 km wide. The vertical extent of this zone can be inferred from the greatest aftershock depths of the Sumatra earthquake (h ~ 60 km).

At the same time, the subvertical fluid-rich zones in the uppermost mantle identified in the areas considered here most likely are discrete spots separated by rock volumes with low concentrations of the liquid phase. The horizontal extent of such spots is probably a few tens of kilometers. Judging by the characteristics of local earthquake codas, high attenuation in the seismicity ring area in Central Tien Shan is observed at depths of ~30–100 km [Bakirov, 2006].

There is comparatively low attenuation inside the seismicity rings in all three areas (the values of Qs are generally much higher than immediately outside the rings). One exception is the source zone of the Kunlun earthquake, along which (*WMQ* data) a narrow band of high attenuation ~400 km long intersecting the seismicity ring passes. The difference in the attenuation field in the eastern part of the source zone based on data from the two stations is probably due to the northward shift in the axis of the high attenuation band relative to the fault zone that accommodated the faulting of the Kunlun earthquake. (The shift of rays due to travel in the uppermost mantle is important here, see Fig. 1.)

The method we used to map lithospheric inhomogeneities does not yield any information on the attenuation field in the crust. However, the seismic data that were previously obtained along with MTS evidence show that fluids in tectonically active areas frequently form a continuous network with connected pores in the lower crust [Van'yan and Hyndman, 1996; Kopnichev and Sokolova, 2007]. If there is a passage from such a network to a similar network in the upper mantle, this leads to stress concentration in highs of the top of the two-phase layer owing to a great difference in the densities of the fluid and the host rocks [Velikhov et al., 2005; Gold and Soter, 1984]. (It is of interest that in this situation the horizontal distance between the "roots" of the two-phase layer in the upper mantle and those in the lower crust is immaterial [Gold and Soter, 1984.) When the two-phase layer is thick enough, its top experiences hydraulic fracture and the fluid rises still higher [Gold and Soter, 1984]. This helps explain the correlation between seismicity characteristics and shear wave attenuation in the areas of ring structures. We note that fluid ascent from the upper mantle is energetically favorable, because it ultimately leads to a decrease of the Earth's potential energy.

As to the factors that favor fluid concentration in the upper mantle in the areas of rings, we suggest the following hypothesis. The low attenuation inside the ring structures makes one think that such locations contain relatively rigid blocks with low concentrations of free fluids. There must be stress concentration at the boundaries of such blocks leading, in particular, to the generation of

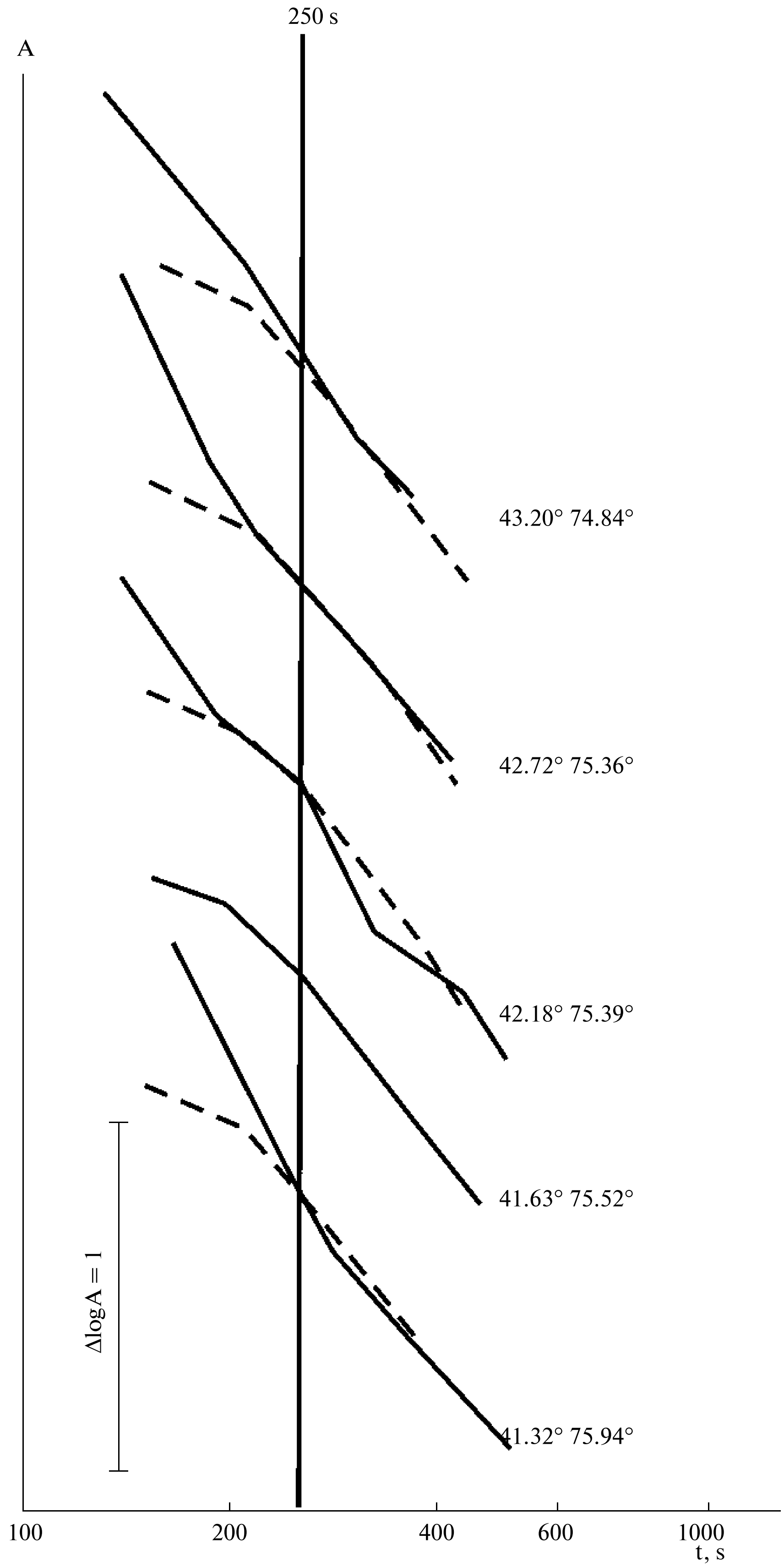

Fig. 16. Sample coda envelopes in the seismicity ring area.
From top to bottom: (1) northwest of the ring, (2, 5) the ring, (3, 4) (and dashed line) inside the ring. *KKAR* data.

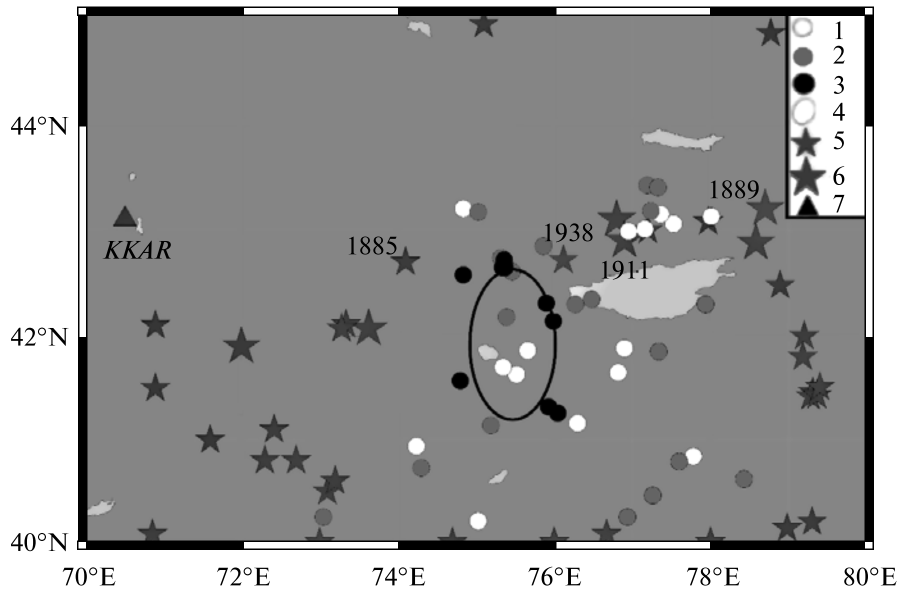

Fig. 17. A map of the attenuation field in Central Tien Shan. Attenuation: (1) low, (2) intermediate, (3) high; (4) seismicity ring. Epicenters of large earthquakes (1885–2007): (5) $6.0 \leq M < 7.0$, (6) $M \geq 7.0$ (with indication of the years of the events mentioned in the text), (7) seismic station.

highly permeable crustal zones [Kocharyan and Spivak, 2003]. In recent years some experimental evidence appeared to show that shear stresses can lead to considerable rearrangement of the fluid field, with the result that fluid that was originally concentrated in the form of isolated bubbles at corners of grains forms a connected network that propagates along their faces [Hier-Majumder and Kohlstedt, 2006; Takei, 2005]. This must lead to the gradual generation of fluid "domains," i.e., vertical channels filled with the liquid phase. As mentioned above, if a domain has a sufficient vertical extent, the domain penetrates beyond the top of the two-phase layer and begins to rise; this is also favored by relatively high rock permeability [Kocharyan and Spivak, 2003].

These results are of importance for seismic zonation and intermediate-term earthquake prediction. The reason for this is that the analysis of seismicity alone can lead to detection of "spurious" rings that are actually unrelated to the precursory processes of large earthquakes (similarly to spurious quiescent zones [Rong et al., 2003]). At the same time, combined use of data on inhomogeneities in the attenuation field will allow a more reliable identification of actual ring structures.

Of special importance is the identification of a ring structure in Central Tien Shan. Comparison with previous data shows that this structure occurs in the northern part of the high attenuation band in the lower crust and upper mantle identified by the analysis of records of deep-focus Hindu Kush earthquakes and the codas of local earthquakes [Bakirov, 2006; Kopnichev and Sokolova, 2007]. Active geodynamic processes are occurring there that seem to be related to the precursory process of a large earthquake [Kopnichev et al., 2004, 2006; Kopnichev and Sokolova, 2007]. It is of interest that, similarly to Sumatra and Tibet, there is a rapid growth in the average rate of seismotectonic strain in Central Tien Shan during recent years. In this connection, as pointed out previously [Kopnichev et al., 2004, 2006; Kopnichev and Sokolova, 2007], work should be carried out in this area to maintain the continuous monitoring of various geophysical and geochemical parameters for the purpose of short-term prediction of a large seismic event.

CONCLUSIONS

(1) It was shown that ring structures consisting of the epicenters of $M \geq 5.5$ events took several decades to form before two great earthquakes, viz., the December 26, 2004 Sumatra and the November 14, 2001 Kunlun earthquakes.

(2) It was found that the ring structures correspond to relatively high attenuation of short period shear waves in the upper mantle. The absence of recent volcanism in the areas of the rings shows that this effect is related to a high concentration of free fluids.

(3) We have identified a ring structure of seismicity in Central Tien Shan that also corresponds to higher attenuation of shear waves. It is hypothesized that the structure is related to the precursory process of a large earthquake in an anomalous zone in North Tien Shan where no large ($M > 6.5$) events have occurred during the last several hundred years.

ACKNOWLEDGMENTS

We are grateful to the IRIS DMC for the digital GSN data they let us use [Butler et al., 2004], as well as to Corresponding Member of the Russian Academy of Sciences

G.A. Sobolev and an anonymous reviewer for helpful remarks.

REFERENCES

Bakirov, A.B., *Zemnaya kora i verkhnyaya mantiya Tyan'-Shanya v svyazi s geodinamikoi i seismichnost'yu* (The Tien Shan Crust and Upper Mantle in Relation to Geodynamics and Seismicity), Bishkek: Ilim, 2006.

Bufe, C., Comparing the November 2002 Denali and November 2001 Kunlun Earthquakes, *Bull. Seismol. Soc. Amer.,* 2004, vol. 94, no. 3, pp. 1159–1165.

Butler, R., Lay, T., Creager, K., et al., The Global Seismographic Network Surpasses Its Design Goals, *EOS Trans. AGU*, 2004, vol. 85, no. 23, pp. 225–232.

Gold, T. and Soter, S., Fluid Ascent through the Solid Lithosphere and Its Relation to Earthquakes, *Pure Appl. Geophys.*, 1984/1985, vol. 122, pp. 492–530.

Hier-Majumder, S. and Kohlstedt, D., Role of Dynamic Grain Boundary Wetting in Fluid Circulation beneath Volcanic Arcs, *Geophys. Res. Lett.,* 2006, vol. 33, L08305.

Jaume, S. and Sykes, L., Evolving towards a Critical Point: A Review of Accelerating Seismic Moment/Energy Release prior to Large and Great Earthquakes, *Pure Appl. Geophys.,* 1999, vol. 155, pp. 279–306.

Kaazik, P.B., Kopnichev, Yu.F., Nersesov, I.L., and Rakhmatullin, M. Kh., An Analysis of Fine Structure in Short Period Seismic Waves Recorded by an Array, *Fizika Zemli,* 1990, no. 4, pp. 38–49.

Kaazik, P.B. and Kopnichev, Yu.F., Numerical Modeling of the Sn Wave Group and Coda in an Earth with Varying Velocity and Attenuation, *Vulkanol. Seismol.*, 1990, no. 6, pp. 74–87.

Kasahara, J., Toriumi, M., and Kawamura, K., *Role of Water in Earthquake Generation, Bull. Earthq. Res. Inst.*, Special Issue, 2001, vol. 76, nos. 3/4.

Kocharyan, G.G. and Spivak, A.A., *Dinamika deformirovaniya blochnykh massivov gornykh porod* (The Dynamics of Deformation in Block Rock Massifs), Moscow: IKTs Akademkniga, 2003.

Kopnichev, Yu.F., *Korotkoperiodnye seismicheskie volnovye polya* (Short Period Seismic Wave Fields), Moscow: Nauka, 1985.

Kopnichev, Yu.F. and Arakelyan, A.R., On the Origin of Short Period Seismic Fields at Distances Less than 3000 km, *Vulkanol. Seismol.*, 1988, no. 4, pp. 77–92.

Kopnichev, Yu.F. and Mikhailova, N.N., Geodynamic Processes in the Rupture Zone of the November 12, 1990 Baisorun Earthquake, Northern Tien Shan, *Dokl. RAN*, 2000, vol. 373, no. 1, pp. 93–97.

Kopnichev, Yu.F. and Sokolova, I.N., Space–Time Variations of the S Wave Attenuation Field in the Rupture Zones of Large Tien Shan Earthquakes, *Fizika Zemli*, 2003, no. 7, pp. 35–47.

Kopnichev, Yu.F. and Sokolova, I.N., Analysis of Space–Time Variations of the Shear Wave Attenuation Field in the Rupture Zones of Large Tien Shan Earthquakes Using Records of Underground Nuclear Explosions, *Dokl. RAN,* 2004, vol. 395, no. 6, pp. 818–821.

Kopnichev, Yu.F., Mikhailova, N.N., and Sokolova, I.N., On the Geodynamic Processes in Central Tien Shan: Identification of an Anomalous Region from Seismic Data, *Vestnik NYaTs RK*, 2004, Issue 3, pp. 111-118.

Kopnichev, Yu.F., Mikhailova, N.N., Sokolova, I.N., and Aristova, I.L., New Evidence Concerning the Geodynamic Processes in the Anomalous Zone of Northern Tien Shan: A Possible Precursory Period of a Large Earthquake, *Vestnik NYaTs RK*, 2006, no. 2, pp. 60–70.

Kopnichev, Yu.F. and Sokolova, I.N., Heterogeneities in the Field of Short Period Seismic Attenuation in the Lithosphere of Central Tien Shan, *Vulkanol. Seismol.*, 2007, no. 5, pp. 54–70 [*Journal of Volcanology and Seismology*, 2007, vol. 1, no. 5, pp. 333–348].

Kopnichev, Yu.F., Gordienko, D.D., and Sokolova, I.N., Space–Time Variations of the Shear Wave Attenuation Field in the Upper Mantle of Seismic and Low Seismicity Areas, *Vulkanol. Seismol.*, 2009, no. 1, pp. 49–64 [*Journal of Volcanology and Seismology*, 2009, vol. 3, no. 1, pp. 44–58].

Krestnikov, V.N., Belousov, T.P., Ermilin, V.I., et al., *Chetvertichnaya tektonika Pamira i Tyan'-Shanya* (Quaternary Tectonics of the Pamirs and Tien Shan), Moscow: Nauka, 1979.

Nakajima, J. and Hasegawa, A., Anomalous Low-Velocity Zone and Linear Alignment of Seismicity along It in the Subducted Pacific Slab beneath Kanto, Japan: Reactivation of Subducted Fracture Zone?, *Geophys. Res. Lett.*, 2006, vol. 33, L16309.

Kondorskaya, N.V. and Shebalin, N.V., *Novyi katalog sil'nykh zemletryasenii na territorii SSSR s drevneishikh vremen do 1975 g.* (A New Catalog of Large Earthquakes in the USSR Area from Earliest Times Until 1975), Moscow: Nauka, 1977.

Rhie, J., Dreger, D., Burgmann, R., and Romanowicz, B., Slip of the Sumatra–Andaman Earthquake from Joint Inversion of Long-Period Global Seismic Waveforms and GPS Static Offsets, *Bull. Seismol. Soc. Amer.*, 2007, vol. 97, no. 1A, pp. S115–S127.

Rong, Yu., Jackson, D., and Kagan, Ya., Seismic Gaps and Earthquakes, *J. Geophys. Res.*, 2003, vol. 108, no. B10, doi: 10.1029/2002JB-002334.

Shchukin, Yu.K., Ryaboi, V.Z., et al., *Glubinnoe stroenie slaboseismichnykh raionov SSSR* (The Deep Structure of Low Seismicity Areas in the USSR), Moscow: Nauka, 1987.

Simoes, M., Avouac, J., Cattin, R., et al., The Sumatra Subduction Zone: A Case for a Locked Fault Zone Extending into the Mantle, *J. Geophys. Res.*, 2004, vol. 109, no. B10, doi: 10.1029/2003JB002958.

Sobolev, G.A., *Osnovy prognoza zemletryasenii* (Principles of Earthquake Prediction), Moscow: Nauka, 1993.

Takei, Ya., Deformation-Induced Grain Boundary Wetting and Its Effects on the Acoustic and Rheological Properties of Partially Molten Rock Analogue, *J. Geophys. Res.,* 2005, vol. 110, no. B12, B12203.

Tapponnier, P. and Molnar, P., Active Faulting and Tectonics in China, *J. Geophys. Res.*, 1977, vol. 82, no. B20, pp. 2905–2930.

Van'yan, L.L. and Hyndman, R.D., On the Origin of Electrical Conductivity in the Consolidated Crust, *Fizika Zemli,* 1996, no. 4, pp. 5–11.

Velikhov, E.P., Golubchikov, L.G., and Karakin, A.V., On the Possibility of Using Electrophysical Methods for Prediction and Modification of Shallow Seismicity, *Dokl. RAN.,* 2005, vol. 401, no. 2, pp. 238–241.

Yamasaki, T. and Seno, T., Double Seismic Zone and Dehydration Embrittlement of the Subducting Slab, *J. Geophys. Res.*, 2003, vol. 109, no. B4, doi: 10.1029/2002JB001918.